



# The role of neighborhood density in the random cellular automata model of grain growth

Michał Czarnecki\* , Mateusz Sitko , Łukasz Madej 

AGH University of Science and Technology, Faculty of Metals Engineering and Industrial Computer Science, al. A. Mickiewicza 30, 30-059 Krakow, Poland.

## Abstract

The paper focuses on adapting the random cellular automata (RCA) method concept for the unconstrained grain growth simulation providing digital microstructure morphologies for subsequent multi-scale simulations. First, algorithms for the generation of initial RCA cells alignment are developed, and then the influence of cells density in the computational domain on grain growth is discussed. Three different approaches are proposed based on the regular, hexagonal, and random cells' alignment in the former case. The importance of cellular automata (CA) cell neighborhood definition on grain growth model predictions is also highlighted. As a research outcome, random cellular automata model parameters that can replicate grain growth without artifacts are presented. It is identified that the acceptable microstructure morphology of the solid material is obtained when a mean number of RCA cells in the investigated neighborhood is higher than ten.

**Keywords:** random cellular automata, grain growth, digital material representation

## 1. Introduction

Complex, multi-scale, full-field numerical models often make direct use of digital microstructure morphology during simulations (Pietrzyk & Madej, 2017; Pietrzyk et al., 2014; Roters et al., 2019). Therefore, the generation of such a digital material representation is of importance (Pietrzyk et al., 2015) and is usually possible with both experimental or numerical-based techniques. The most straightforward microstructure replication approaches are based on experimental data (Madej, 2017). In that case, the preparation of the digital microstructure model is based on metallographic images from light or electron microscopy since in that way 2D material models are easily created (Liu et al., 2017). For the generation of 3D representation, a set of serial sectioning

data can be used (Madej et al., 2018a), but this approach requires significant time and resources. Conventionally different techniques utilize X-ray tomography (Pokharel et al., 2015), providing precise information about material morphology, phases, and even energy accumulation in the material. In the latter case, the problem is still related to a relatively small volume of the investigated sample. Therefore, a series of numerical approaches are frequently used as a supplementary method to experimental research because of the aforementioned difficulties. Different numerical approaches for the generation of the digital material representation models are available in the literature, e.g., Monte Carlo method (Maazi & Lezzar, 2020), Voronoi tessellation (Falco et al., 2017), phase field (Tegeler et al., 2017) or cellular automata (CA) methods (Hajder & Madej, 2020).

\* Corresponding author: [czarnecky@va.pl](mailto:czarnecky@va.pl)

ORCID ID's: 0000-0001-8236-8578 (M. Czarnecki), 0000-0003-0893-8784 (M. Sitko), 0000-0003-1032-6963 (Ł. Madej)

© 2021 Authors. This is an open access publication, which can be used, distributed and reproduced in any medium according to the Creative Commons CC-BY 4.0 License requiring that the original work has been properly cited.

As mentioned earlier, one of the methods that allows the digital replication of even highly complex heterogeneous microstructures is the cellular automata approach. The classical and frontal CA variants were developed, and they provide possibilities for the generation of various microstructure types both in 2D and 3D space (Svyetlichnyy, 2013). The classical CA grain growth model, is based on a regular fixed space with CA cells aligned in the hexagonal-based (Fig. 1a) (Owusu et al., 2019), square-based grids (Boguń et al., 2021) (Fig. 1c), or other different regulars ones like circular or octagonal (Fig. 1b). The drawback of this classical approach is that the morphology of the grains is affected by the CA space isotropic character. When random definitions of the CA neighborhood are considered (Groß et al., 2019), this issue is significantly suppressed. However, CA cells regular distribution within the computational domain generates another difficulty when more advanced coupled approaches like concurrent cellular automata in finite element models are considered (Shterenlikht et al., 2018, Szyndler & Madej, 2015). In this case, the finite element meshes are usually unstructured or even anisotropic, and direct data transfer between the CA space and FE mesh is not straightforward. This is especially problematic in predicting more complex microstructure evolution models, e.g., dynamic recrystallization or fracture, where both computational domains undergo shape change due to plastic deformation (Li et al., 2016). To eliminate these difficulties, a random cellular automata (RCA) concept (Fig. 1d) can be used as presented in work by Madej et al. (2018b).

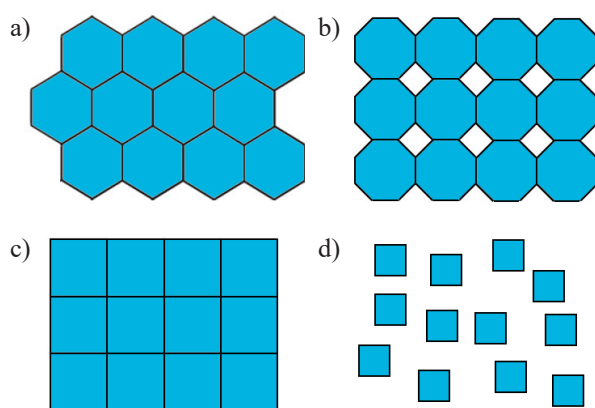


**Fig. 1.** Cells alignment in the computational domain for the classical CA method with hexagonal (a), octagonal (b), square grids (c) and random (d) CA method

However, the algorithmic complexity of the random CA approach increases with respect to classical CA, and also, the model predictions can be significantly

affected by the setup parameters (e.g., the density of CA cells, type of neighborhood, neighborhood radius etc.), leading to unphysical predictions. Therefore, developing a simple but computationally efficient grain growth algorithm within the RCA concept and further evaluating the role of the setup parameters is the current research goal. The knowledge obtained will allow for the further application of this concept to more complex microstructure evolution models, e.g., dynamic recrystallization. In this case, the CA space deformation can be captured during the simulations and thus overcoming a major limitation of the classical CA method.

## 2. Random cellular automata grain growth model

In the RCA approach, computations are realized in a mesh-free environment within the cloud of CA cells. Therefore, each simulation requires an initial distribution of cells across the computational domain. When coupled with other computational techniques such as the finite element method, the CA cell positions can be obtained directly from the finite element mesh. However, if stand-alone RCA calculations are investigated, then a position of each CA cell has to be generated by a dedicated distribution algorithm. The distribution pattern of cells is essential and can affect the simulation's final result, especially the grain boundary shapes. Within the work, three different approaches for CA cell distribution were investigated: regular, hexagonal, and random, as seen in Figure 2. Each CA cell can take two states in the model: empty and non-empty. The cell in the later state is also identified by an id number, which represents its assignment to a particular grain, visualized further by different colors.

After the initial distribution of CA cells in the computational domain and the execution of the nucleation phase (selected number of cells change the state to non-empty and unique color is assigned to each of them), the grain growth algorithm is initiated. In the first step of each iteration, for a selected cell in the state empty, all non-empty neighbors are identified according to the defined neighborhood type. As mentioned in the RCA method, various types of neighborhoods can be proposed. However, in each case, the neighbors are always determined with respect to the position of the investigated CA cell. Besides the classical circular neighborhood shape (Fig. 3a), more sophisticated ones like elliptical or complex neighborhood shape definitions are also proposed within the work, as seen in Figure 3b and 3c.

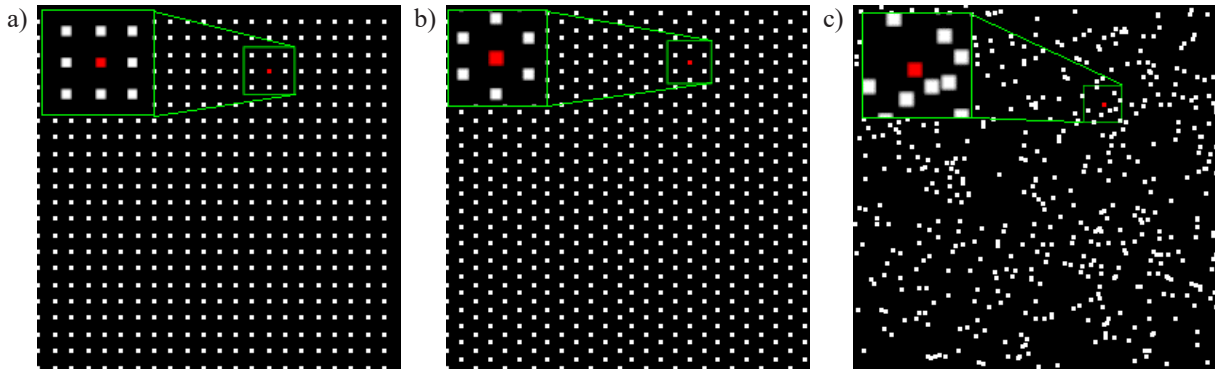


**Fig. 2.** Different CA cell distribution algorithm outputs: a) regular; b) hexagonal; c) random (white point represents empty cells while colored one new nuclei in the CA space)

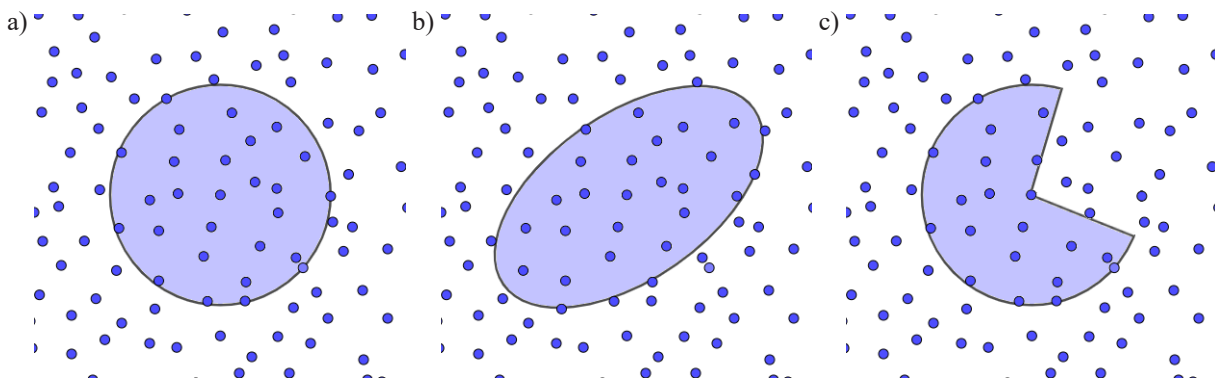


**Fig. 3.** Different shapes of the RCA neighborhood: a) circular; b) elliptical; c) complex

Then, in the second step, based on one of the neighboring ids, a new id for the investigated cell is selected, and the cell changes the state to non-empty. The algorithm operates until all CA cells change their state to non-empty.

It should be stressed that the presented approach is sensitive to evaluating CA neighbors' order and size of applied neighborhood radius, which may lead to the unrealistic representation of grain morphology. As seen in Figure 4a, when first encountered, neighbor id is trans-

ferred to the investigated CA cell then the final microstructure is far from expectation. This problem can be mostly reduced by the application of different transition rules such as those presented in Figure 4b when the most common id from all the neighbors is assigned to the investigated cell. Yet in this case, some problems can still appear when a large radius of the neighborhood is selected. During the research, it was identified that to eliminate such artifacts, only the id of the closest neighbor should be assigned to the investigated CA cell (Fig. 4c).

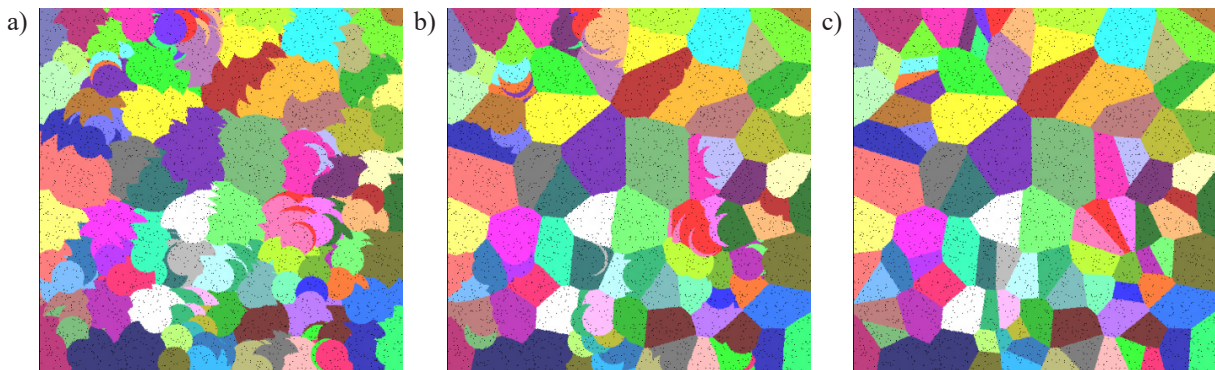


**Fig. 4.** Effects of different methods for a new id selection for an empty cell: a) the first encountered id; b) id most often occurring in the neighborhood; c) id from the closest neighbor

The other disadvantage of the RCA approach is that the evaluation of CA cell along with its neighborhood in subsequent iterations is computationally costly because each cell has to be checked against all other cells within the computational domain. To decrease the time of the neighborhood search, a bounding box algorithm (Walizer & Peters, 2011) that can be easily used for various types of neighborhood types was adapted for the current work (Fig. 5).

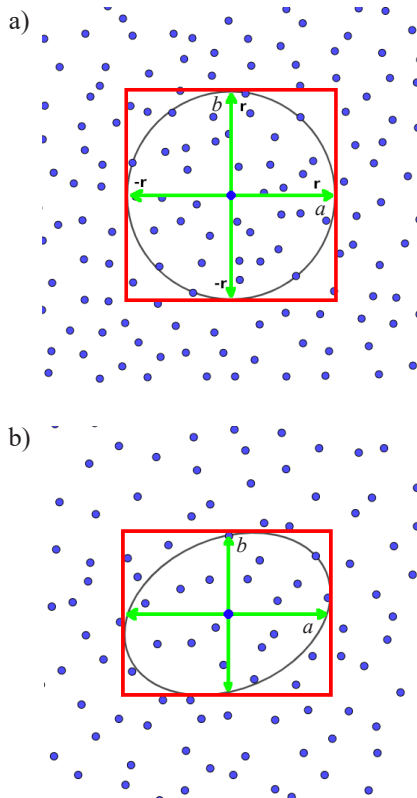


**Fig. 5.** Example of the bounding box for circular (a) and elliptical (b) neighborhood type

Additionally, to reduce computing times, the only interaction between CA cells in the state empty  $\leftarrow$  non-empty is considered. All other interactions of CA cells in the following states and configurations: empty cell  $\leftarrow$  empty neighbors, non-empty cell  $\leftarrow$  empty neighbors, non-empty cell  $\leftarrow$  non-empty neighbors are neglected as they have no influence on the final results.

Examples of results obtained from the developed random cellular automata grain growth algorithm for various initial RCA cell distributions are shown in Figures 6–8. In all case studies, the same number of grain nuclei equal to 200 was distributed across the computational domain with one million cells. The physical size of the investigated microstructures was set to  $100 \times 100 \mu\text{m}$ .

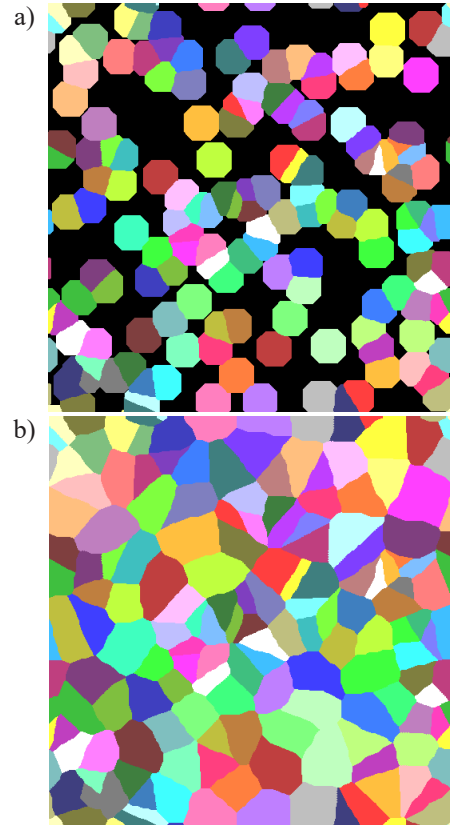


**Fig. 6.** Grain growth within the RCA space with regular cells distribution after 10 (a) and 31 (b) iterations

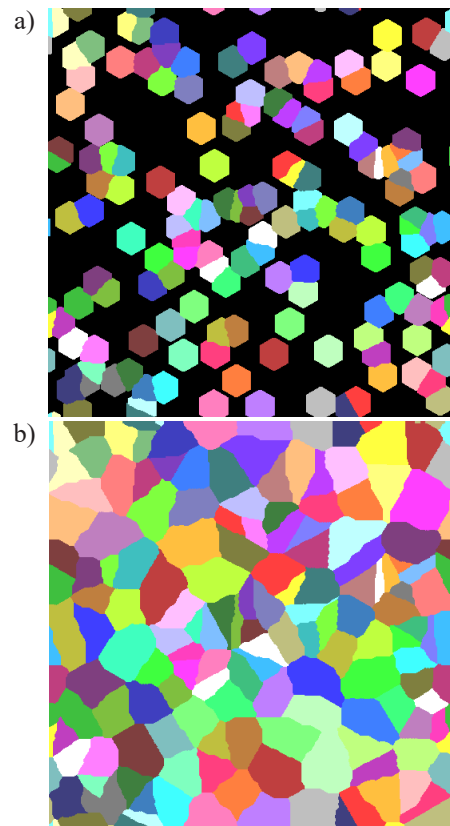


**Fig. 7.** Grain growth within the RCA space with hexagonal cells distribution after 18 (a) and 64 (b) iterations

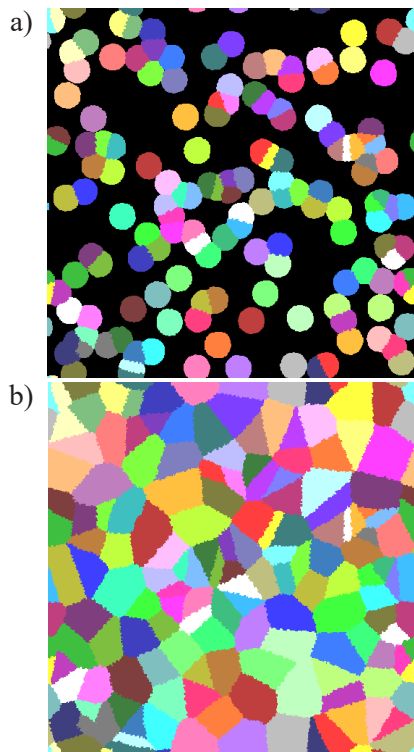


**Fig. 8.** Grain growth within the RCA space with the random cells distribution after 8 (a) and 30 (b) iterations

As presented, the type of initial cell distribution can slightly affect the shape of the growing grains and final microstructure morphology. However, in this case, the most critical parameter is the neighborhood type used during simulation that has a significant impact on the shape of growing grains. This is very beneficial in some cases, where, e.g., equiaxial grains are not desired, and other microstructure morphologies are required for numerical simulations, e.g., with elongated grains. In such a case, the elliptical neighborhood (Fig. 3b) definition can be used. The two radii and alignment angle describe such a neighborhood to reflect elongation in any given direction, as seen in (Figs. 9 and 10). Moreover, during a simulation, the parameters of the neighborhood can be modified, as presented in Figure 11. In this case, a random angle of rotation is assigned to investigated RCA cells at the beginning of each time step, and the evolution of grain shapes changes significantly as a result.

As pointed out in the RCA method, more complex, non-standard neighborhood shapes can also be easily incorporated. Examples of numerical simulations with a neighborhood definition from Figure 3c are shown in Figure 12.

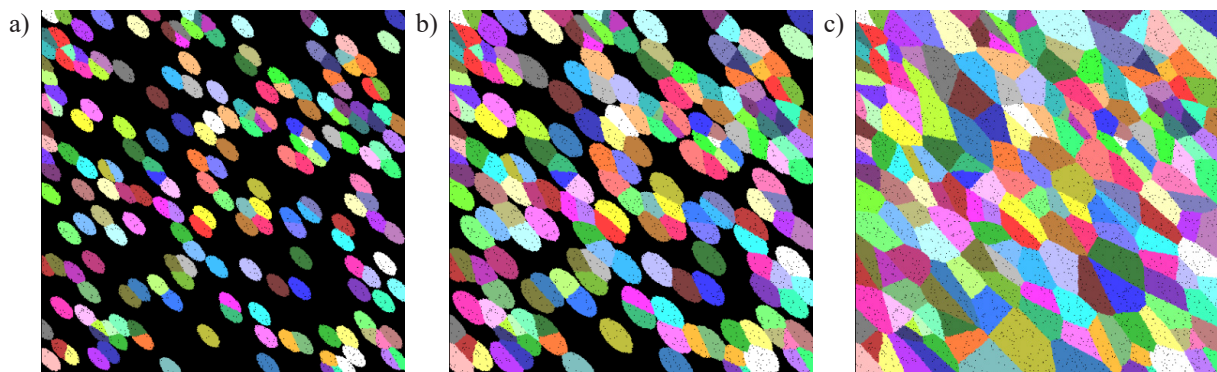


**Fig. 9.** Grain growth with the elliptical neighborhood and the radii:  $a = 0.45 \mu\text{m}$ ,  $b = 0.225 \mu\text{m}$ , rotated by  $45^\circ$ , after 10 (a), 15 (b), 40 (c) iterations

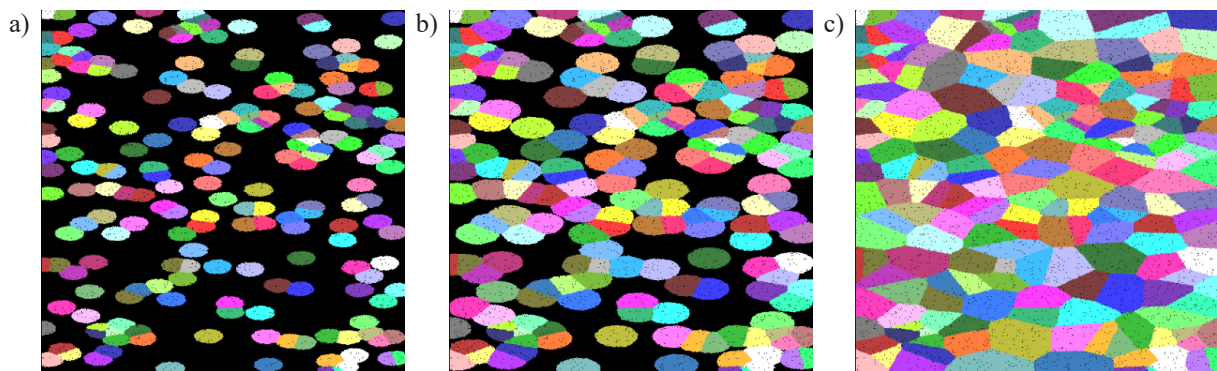


**Fig. 10.** Grain growth with the elliptical neighborhood and the radii:  $a = 0.45 \mu\text{m}$ ,  $b = 0.225 \mu\text{m}$ , without rotation, after 10 (a), 15 (b), 36 (c) iterations

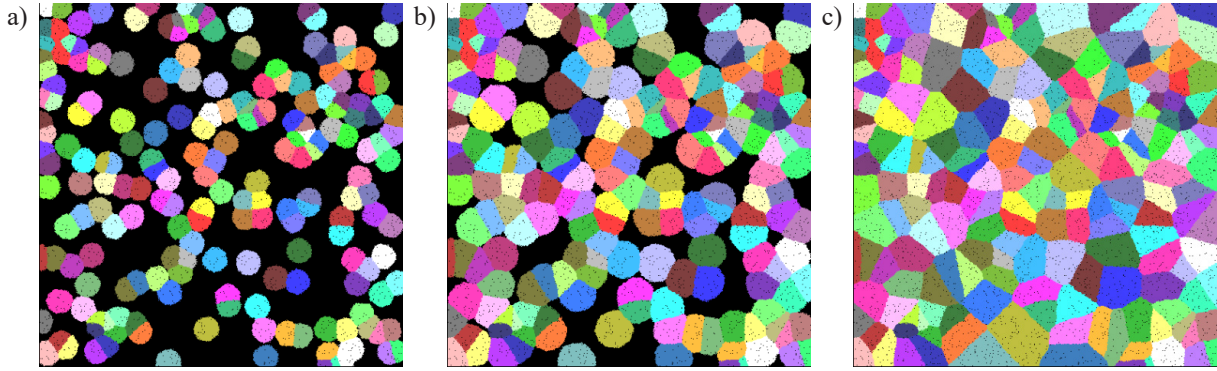


**Fig. 11.** Grain growth with the elliptical neighborhood and the radii:  $a = 0.45 \mu\text{m}$ ,  $b = 0.225 \mu\text{m}$ , with random rotations, after 10 (a), 15 (b), 34 (c) iterations

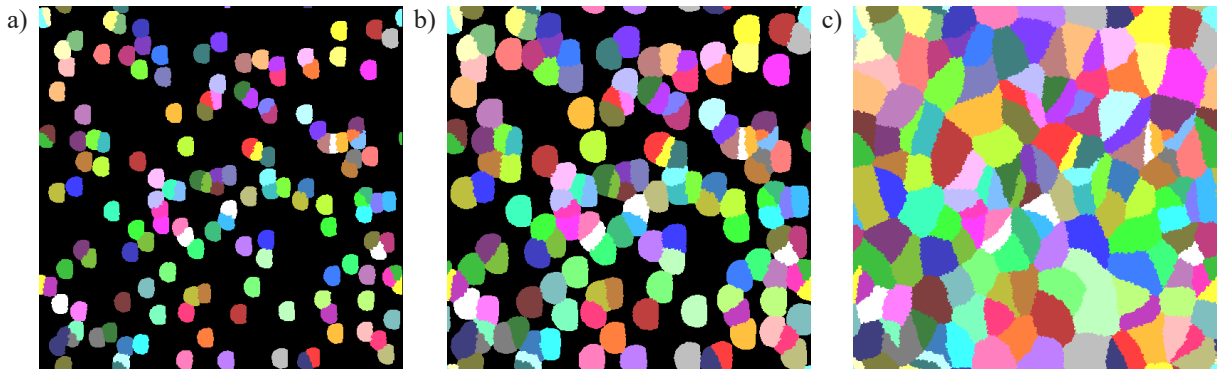


**Fig. 12.** Grain growth with a custom definition of the neighborhood after 6 (a), 10 (b), and 32 (c) iterations

### 3. Parametrization of the model

The RCA grain growth algorithm's simulation setup parameters compose the number of cells, their spatial distribution, the type and size of the neighborhood, e.g., the radius in a circular type neighborhood. It is worth noting that these parameters alone may be misleading. Therefore, it is worth normalizing them for the sake of the current study. Since the cells' distribution in the simulation is random or uniform, determination of the mean density  $\bar{\rho}$  and the mean number of cells  $\bar{N}$  in the neighborhood defined by radius  $r$  can be done as follow:

$$\bar{\rho} = \frac{n}{s} \quad (1)$$

where:  $n$  – the overall number of cells in the computational domain;  $s$  – physical space area.

$$\bar{N} = \bar{\rho}\pi r^2 \quad (2)$$

The inappropriate selection of the initial setup parameters can affect grain growth, leading to unphysical microstructure morphology of the solid material, as seen in Figure 13 for the case of  $\bar{N} = 4.5$  and two different overall numbers of cells in the computational domain (physical space size  $100 \times 100 \mu\text{m}$ ).

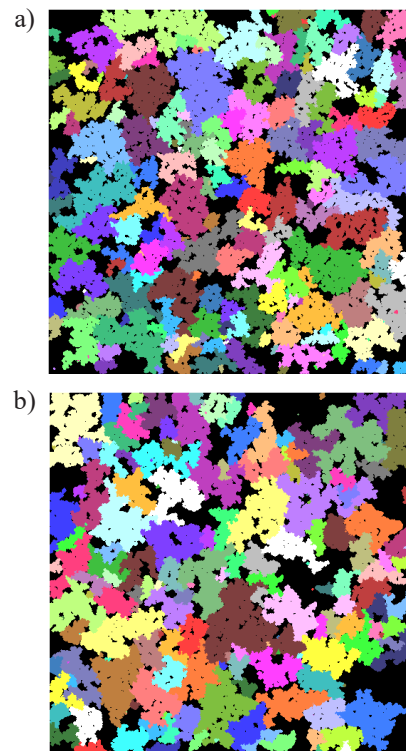


**Fig. 13.** Simulation for  $\bar{N} = 4.5$  and a different number of cells in the computational domain: a)  $5e5$  cells,  $r = 0.169 \mu\text{m}$ ; b)  $2.5e6$  cells,  $r = 0.0755 \mu\text{m}$

Therefore, as presented, identifying the proper setup parameters is critical for the RCA grain growth predictions. For the unconstrained grain growth, depending on  $\bar{N}$  value, the simulation can provide satisfactory or totally not physical results for the solid material. However, it should be pointed out that sometimes the behavior from Figure 13 can be valuable, e.g., to reconstruct the morphology of porous sintered microstructure, but this is beyond the scope of this paper. To evaluate the proper  $\bar{N}$  value for solid material, a set of simulations with increasing  $r$  size (0.27640–1.04366  $\mu\text{m}$ ) and a number of cells (25,000–175,000 cells) was computed. During each simulation, precisely the same physical size of space equal to  $100 \times 100 \mu\text{m}$  was analyzed, and the same number of 100 nuclei were distributed in similar physical locations. Results from such simulations are presented in Figure 14.

As can be noticed in Figure 14, when the parameter  $\bar{N}$  is around 1–4, then there are approximately 1–4 cells on average in the neighborhood, including the investigated CA cell. With such density, only a few initial grains will grow during the simulation. For higher values of  $\bar{N}$  around 6 (Fig. 14), larger grains are formed, but there are still some small empty areas between the grains. Then, for the value of  $\bar{N} > 10$  (Fig. 14), the majority of the space between the grains is filled, the black areas are negligible. However, it should also be pointed out that, even for a sufficiently large number of CA points in the model, there may be situations when the black regions remain, even if 100% of cells have assigned id and color. This is purely related to the random distribution of the CA points in a fixed physical region ( $100 \times 100 \mu\text{m}$ ).

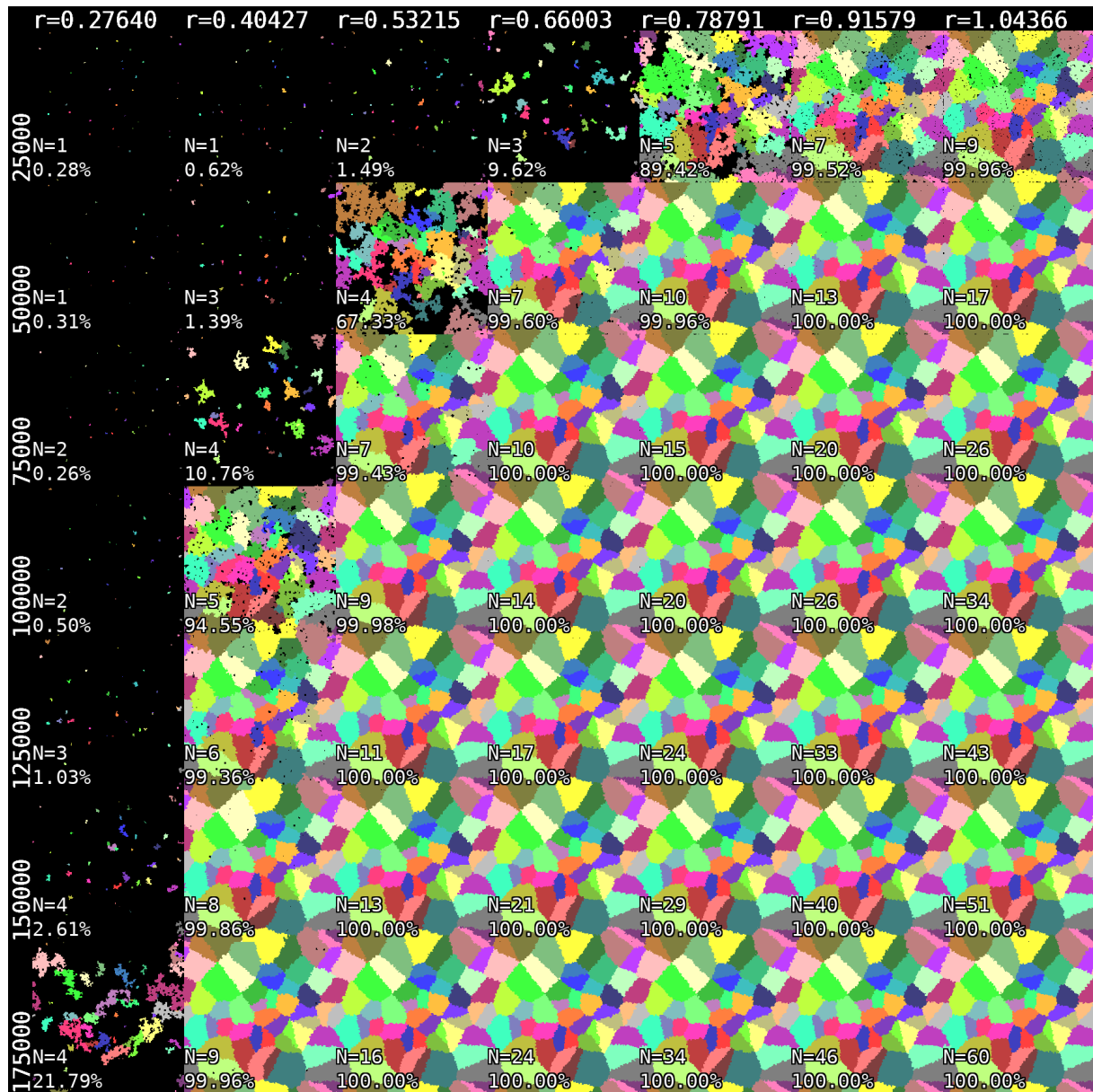


Fig. 14. Comparison of simulation results using increasing cells number from 25,000 to 175,000 with increasing radius values from 0.27640  $\mu\text{m}$  to 1.04366  $\mu\text{m}$

## 4. Conclusions

The adaptation of the random cellular automata (RCA) method concept for the unconstrained grain growth simulation providing digital microstructure morphologies for subsequent simulations was performed. The investigation of the model setup parameters on the final results in the form of digital microstructure morphologies was performed and delivered the following conclusions:

- Various CA cell alignments, including fully random, can be used during grain growth simulations. The fully random CA cell distribution is important as such a model can be directly linked with unstructured finite element meshes during coupled CA-FE calculations.
- The assumptions of the RCA approach ensure that even complex types of user-defined neighborhoods can be used during the simulations,

which increases the model flexibility in application to the generation of various microstructure morphologies.

The selection of initial parameters is of importance to provide the required digital morphology. For circular neighborhood and small value of  $\bar{N}$ , only a small amount of cells during simulation can obtain an id number and represent the grain. The acceptable microstructure morphology of the solid material is obtained with the  $\bar{N} > 10$ . At the same time, intermediate  $\bar{N}$  values can be used to generate digital microstructures of, e.g., some porous materials.

## Acknowledgment

The financial assistance of the National Science Centre project No. 2019/35/B/ST8/00046 is acknowledged.

## References

- Boguń, K., Sitko, M., Mojżeszko, M., & Madej, Ł. (2021). Cellular Automata-based computational library for development of digital material representation models of heterogenous microstructures. *Archives of Civil and Mechanical Engineering*, 21(2), 61. <https://doi.org/10.1007/s43452-021-00211-9>.
- Falco, S., Jiang, J., De Cola, F., & Petrinic, N. (2017). Generation of 3D polycrystalline microstructures with a conditioned Laguerre-Voronoi tessellation technique. *Computational Materials Science*, 136, 20–28. <https://doi.org/10.1016/j.comatsci.2017.04.018>.
- Groß, J., Köster, M., & Krüger, A. (2019). Fast and Efficient Nearest Neighbor Search for Particle Simulations. In: *Computer Graphics and Visual Computing (CGVC) 2019, 12<sup>th</sup>–13<sup>th</sup> September 2019, Bangor University, United Kingdom*, 55–63. <https://doi.org/10.2312/cgvc.20191258>.
- Hajder, L., & Madej, Ł. (2020). Sphere Packing Algorithm for the Generation of Digital Models of Polycrystalline Microstructures with Heterogeneous Grain Sizes. *Computer Methods in Materials Science*, 20(1), 22–30. <https://doi.org/10.7494/cmms>.
- Li, H., Sun, X., & Yang, H. (2016). A three-dimensional cellular automata-crystal plasticity finite element model for predicting the multiscale interaction among heterogeneous deformation, DRX microstructural evolution and mechanical responses in titanium alloys. *International Journal of Plasticity*, 87, 154–180. <https://doi.org/10.1016/j.ijplas.2016.09.008>.
- Liu, J., Dai, Q., Chen, J., Chen, S., Ji, H., Dua, W., Deng, X., Wang, Z., Guo, G., & Luo, H. (2017). The two dimensional microstructure characterization of cemented carbides with an automatic image analysis process. *Ceramics International*, 43(17), 14865–14872. <https://doi.org/10.1016/j.ceramint.2017.08.002>.
- Maazi, N., & Lezzar, B. (2020). An efficient Monte Carlo Potts method for the grain growth simulation of single-phase systems. *Computer Methods in Material Science*, 20(3), 85–94. <https://doi.org/10.7494/cmms.2020.3.0722>.
- Madej, L. (2017). Digital/virtual microstructures in application to metals engineering – A review. *Archives of Civil and Mechanical Engineering*, 17(4), 839–854. <https://doi.org/10.1016/j.acme.2017.03.002>.
- Madej, L., Legwand, A., Mojżeszko, M., Chraponski, J., Roskosz, S., & Cwajna, J. (2018a). Experimental and numerical two- and three- dimensional investigation of porosity morphology of the sintered metallic material. *Archives of Civil and Mechanical Engineering*, 18(4), 1520–1534. <https://doi.org/10.1016/j.acme.2018.06.007>.
- Madej, L., Sitko, M., Legwand, A., Perzynski, K., & Michalik, K. (2018b). Development and evaluation of data transfer protocols in the fully coupled random cellular automata finite element model of dynamic recrystallization. *Journal of Computational Science*, 26, 66–77. <https://doi.org/10.1016/j.jocs.2018.03.007>.
- Owusu, P.A., Leonenko, V.N., Mamchik, N.A., & Skorb, E.V. (2019). Modeling the growth of dendritic electroless silver colonies using hexagonal cellular automata. *Procedia Computer Science*, 156, 43–48. <https://doi.org/10.1016/j.procs.2019.08.128>.
- Pietrzyk, M., & Madej, L. (2017). Perceptive Review of Ferrous Micro/Macro Material Models for Thermo-Mechanical Processing Applications. *Steel Research International*, 88(10). <https://doi.org/10.1002/srin.201700193>.
- Pietrzyk, M., Kusiak, J., Kuziak, R., Madej, L., Szelięga, D., & Gołąb, R. (2014). Conventional and Multiscale Modeling of Microstructure Evolution During Laminar Cooling of DP Steel Strips. *Metallurgical and Materials Transactions A: Physical Metallurgy and Materials Science*, 45(13), 5835–5851. <https://doi.org/10.1007/s11661-014-2393-z>.
- Pietrzyk, M., Madej, L., Rauch, L., & Szelięga, D. (2015). *Computational Materials Engineering: Achieving High Accuracy and Efficiency in Metals*. Elsevier Science.

- Pokharel, R., Lind, J., Li, S.F., Kenesei, P., Lebensohn, R.A., Suter, R.M., & Rollett, A.D. (2015). In-situ observation of bulk 3D grain evolution during plastic deformation in polycrystalline Cu. *International Journal of Plasticity*, *67*, 217–234. <https://doi.org/10.1016/j.ijplas.2014.10.013>.
- Roters, F., Diehl, M., Shanthraj, P., Eisenlohr, P., Reuber, C., Wong, S.L., Maiti, T., Ebrahimi, A., Hochrainer, T., Fabritius, H.O., Nikolov, S., Friák, M., Fujita, N., Grilli, N., Janssens, K.G.F., Jia, N., Kok, P.J.J., Ma, D., Meier, F., Werner, E., Stricker, M., Weygand, D., & Raabe, D. (2019). DAMASK – The Düsseldorf Advanced Material Simulation Kit for modeling multi-physics crystal plasticity, thermal, and damage phenomena from the single crystal up to the component scale. *Computational Materials Science*, *158*, 420–478. <https://doi.org/10.1016/j.commatsci.2018.04.030>.
- Shterenlikht A., Margetts L., & Cebamano L. 2018. Modelling fracture in heterogeneous materials on HPC systems using a hybrid MPI/fortran coarray multi-scale CAFE framework, *Advances in Engineering Software*, *125*, 155–166. <https://doi.org/10.1016/j.advengsoft.2018.05.008>.
- Svyetlichnyy, D.S. (2013). Modeling of grain refinement by cellular automata. *Computational Materials Science*, *77*, 408–416. <https://doi.org/10.1016/j.commatsci.2013.04.065>.
- Szyndler, J., & Madej, Ł. (2015). Numerical analysis of the influence of number of grains, FE mesh density and friction coefficient on representativeness aspects of the polycrystalline digital material representation – Plane strain deformation case study. *Computational Materials Science*, *96*(pt. A), 200–213. <https://doi.org/10.1016/j.commatsci.2014.08.037>.
- Tegeler, M., Shchyglo, O., Kamachali, R.D., Monas, A., Steinbach, I., & Sutmann, G. (2017). Parallel multiphase field simulations with OpenPhase. *Computer Physics Communications*, *215*, 173–187. <https://doi.org/10.1016/j.cpc.2017.01.023>.
- Walizer, L.E., & Peters, J.F. (2011). A bounding box search algorithm for DEM simulation. *Computer Physics Communications*, *182*(2), 281–288. <https://doi.org/10.1016/j.cpc.2010.09.008>.

